Fourier Amplitude Spectrum at Arbitrary Points Estimated by Kriging Method

Yukari Mizutani
Obayashi Corporation, M. Eng., Japan

Michiyo Sugai
Prof., Dept. of Environmental Management, Grad. School of Nagoya Sangyo Univ., Dr. Eng., Japan

Yasuhiro Mori
Prof., Dept. of Environmental Engineering and Architecture, Nagoya Univ., Ph.D., Japan

ABSTRACT: This paper reports a method for estimating an acceleration Fourier amplitude spectrum (FS) on ground surface at arbitrary points using the transfer functions of the surface strata and the observation records of limited number of seismometers. The transfer functions at arbitrary points in Owari-asahi City are estimated by using a modified Kriging method based on the results of the seismic response analysis of the surface strata at 748 boring points using seismic waves on engineering bedrock caused by six earthquake scenarios. The acceleration FS on the surface at 642 boring points inside the city are estimated by using the proposed method based on only 20 observation records on the surface (estimated value). The result is compared to the acceleration FS estimated by the transfer functions and seismic waves on the engineering bedrock from earthquake scenarios at the same boring points (tentative observed value). It is found that the correlation coefficients per frequency between the estimated and tentative observed value at 642 points are no less than 0.5 any earthquake scenario.

To date, earthquake ground motion intensities (GMIs) have been estimated for predefined meshes with fixed sides of lengths of 50 m, 250 m, or 500 m using hypothetical ground models created on the basis of boring investigation data. However, to employ effective measures for seismic damage mitigation and contribute to a resilient society, the GMI should be estimated in greater detail, such as at each construction site. In order to do so, Sugai et al. (2015) proposed a modified Kriging method that can take into account for non-negligible errors in the estimations of the spatial distributions of the GMIs at boring points. The method has already been applied to the estimations of seismic hazards and risks using earthquake scenarios in Owari-asahi City, Aichi prefecture, Japan.

Expanding the above method, it should be possible to estimate the GMI at an arbitrary point using observation records of limited number of seismometers. However, it is practically impossible to estimate the spatial distribution of the GMI on the surface directly from the observation records on the surface. For example, in Owari-asahi City, it is necessary approximately one seismometer for every 100 m^2 to estimate the GMI at an arbitrary point on the surface, considering that the auto-correlation distances for the GMI (PGA, PGV and instrumental seismic intensity) on the surface are approximately 150–700 m in the city (Sugai et al. 2016).

In contrast, the auto-correlation distances for the GMI on engineering bedrock are much longer approximately 1.5–2 km in the city (Mizutani et al. 2017). Accordingly, the GMI on the surface at an arbitrary point could be estimated by an amplification factor and the spatial distribution of the seismic wave on the engineering bedrock at the same point, which is estimated by using the modified Kriging method based on seismic waves on the engineering bedrock at seismometer points by using seismic response analysis of surface strata based on the observation records, requiring approximately one seismometer for every 1 km^2 on the surface. However, the amplification factor of the GMI depends not only on the characteristics of the surface strata, but also on the frequency characteristics of earthquake ground motion.

This paper demonstrates estimating an acceleration Fourier amplitude spectrum (FS) on ground surface at an arbitrary point using a transfer function of surface strata and observation records of limited number of seismometers in Owari-asahi City. Using the acceleration FS, it is possible to calculate an acceleration response spectrum (AIJ 2015) to estimate seismic damage. At first, the authors calculated the transfer function at an arbitrary point by using the modified Kriging method based on the transfer function at boring points and earthquake scenarios. The transfer function at a boring point is calculated by using seismic response analysis of surface strata based on input seismic wave on the engineering bedrock from earthquake scenarios. Also, the authors compare the acceleration FS by the proposed method at the boring points with those estimated by the transfer functions and seismic waves on the engineering bedrock for earthquake scenarios at the same boring points.

1. PROPOSED METHOD

1.1. A transfer function at a boring point

An acceleration FS on ground surface, $A^O(f)$, is identified as (Iwata and Irikura 1986),

$$A^O(f) = A^E(f) \cdot A^G(f) \quad (1),$$

in which $A^E(f)$ is an acceleration FS on engineering bedrock and $A^G(f)$ is transfer function at an observation point. $A^G(f)$ at an arbitrary point could be estimated by using the modified Kriging method based on the spectral ratios of $A^O(f)$ to $A^E(f)$ at boring points.

To estimate the transfer function and the acceleration FS on the surface at the boring points, the authors used equivalent linear analysis and equivalent strain frequency dependencies (Sugito et al. 1994) because it is necessary to pull back the observation records on the surface to the engineering bedrock. The acceleration FS on the surface at boring points were calculated by using one-dimensional seismic response analysis based on input seismic wave on the engineering bedrock from earthquake scenarios. The dynamic shear modulus (G-γ) and damping (h-γ) used the model of the seismic response analysis is identified as (Imazu and Fukutake 1986a), respectively,

Table 1: Parameters for Eqs. (2) and (3)

	Sand	Cohesive Soil	Gravel
a	729.7	179.1	392.8
b	0.89	0.79	0.75
c	338.0	46.84	75.36
d	0.47	0.27	0.30
e	111.30	94.38	123.05
f	0.3020	0.3144	0.2443

$$\frac{G}{G_{max}} = \frac{1}{(1 + a(\gamma) \cdot b)}, \quad h = c(\gamma) \cdot d \quad (2),$$

in which G/G_{max} is the shear ratio, h is the attenuation coefficient (%), γ is the shearing strain, and a, b, c, and d are the parameters of each soil (Imazu and Fukutake 1986b) of the boring data in Table 1. The velocity of the secondary wave, *Vs* (m/s), is identified as (Cabinet Office, Government of Japan 2005),

$$V_s = e \times Nf \quad (3),$$

where N is the average value of N each surface strata of the boring data, and e and f are the parameters of each soil in Table 1. The authors assume that the range of the maximum strain levels of the surface strata is effective to within approximately 0.1% (Yoshida 2010). The acceleration FS on the surface and the engineering bedrock are both smoothed in a Parzen window with a bandwidth of 0.4 Hz.

1.2. A modified Kriging method

The transfer function at an arbitrary point could be estimated per frequency by using the modified Kriging method based on the transfer function at boring points in Section 1.1. An overview of the modified Kriging method (Sugai et al. 2015) is provided below.

To estimate the spatial distribution of a parameter by using the Kriging method based on a set of field data, it is necessary to identify a variogram and trend function. A variogram is the covariance matrix of a random field model and a trend function represents the overall tendency within the field (Krige 1951; Matheron 1963).

The optimal random field model (i.e., the optimal variogram and trend function) for the spatial distribution of GMI is identified as a model with a minimum Akaike Information Criterion (AIC) (Akaike 1973) based on the general maximum likelihood method as

$$\min_{\boldsymbol{\mu},\boldsymbol{\theta},m} \mathbf{AIC} = -2 \times \mathrm{Max}\{\ln p(\mathbf{z}|\boldsymbol{\mu},\boldsymbol{\theta})\} + 2 \times (m) \tag{4}$$

in which $\mathbf{z}$ is the vector of GMIs, and m denotes the number of random field explanatory variables. In addition, $p(\mathbf{z}|\cdot)$ is a multivariate probability density function of $\mathbf{z}$ with parameters $\cdot$. It is often modeled by a joint normal probability density function as

$$p(\mathbf{z}|\boldsymbol{\mu},\boldsymbol{\theta}) = \left(\frac{1}{\sqrt{2\pi}}\right)^{\frac{n}{2}} \frac{1}{|\mathbf{z}|} |\mathbf{C}|^{-\frac{1}{2}} \exp\left\{-\frac{1}{2}(\ln(\mathbf{z}) - \boldsymbol{\mu})^T \mathbf{C}^{-1}(\ln(\mathbf{z}) - \boldsymbol{\mu})\right\} \tag{5}$$

in which $\boldsymbol{\theta}$ denotes the explanatory variables of $\mathbf{C}$, which is the covariance matrix of $\mathbf{z}$, and n is the number of the acquired data. $\boldsymbol{\mu}$ is the average value vector determined by the trend function of $\mathbf{z}$ (Wackernagel 2011). It can also be expressed as function of the maximum degree, n_t, of the coordinate $\mathbf{u} = (x, y)$ (Honda 2000) as

$$\begin{aligned}\mu(\mathbf{u}_i) = \mathbf{b} \cdot \mathbf{f}(\mathbf{u}_i) &= \sum_{k=0}^{m_t-1} b_k f_k(\mathbf{u}_i) = \sum_{k=0}^{m_t-1} b_k f_k(x_i, y_i) \\ &= b_0 + b_1 x_i + b_2 y_i + b_3 x_i^2 + b_4 x_i y_i + b_5 y_i^2 + \cdots \\ &+ b_{m_t-2} x_i y_i^{n_t-1} + b_{m_t-1} y_i^{n_t}\end{aligned} \tag{6}$$

in which $\mathbf{f}(\mathbf{u})$ is the vector of the location, $\mathbf{b}$ is the coefficient vector, and m_t denotes the number of elements in $\mathbf{b}$. Furthermore, m_t can be expressed by n_t of Eq. (6) as

$$m_t = \frac{(n_t + 1)(n_t + 2)}{2} \tag{7}$$

The i and j elements of the covariance matrix $\mathbf{C}$ in Eq. (5), $C(\mathbf{u}_i, \mathbf{u}_j)$, denote the covariance of GMIs between the two points i and j, which have the coordinates of $\mathbf{u}_i$ and $\mathbf{u}_j$, respectively. It depends only on the distance, h, between these two points. The elements can be expressed as a general exponential model as

$$C(\mathbf{u}_i, \mathbf{u}_j) = C(h) = \sigma^2 \exp\left(-\frac{h}{\ell}\right) \tag{8}$$

in which σ^2 and ℓ are the parameters of the sill and range, respectively. The covariance function can be modified for anisotropic random fields (Wackernagel 2011), and zoning method or others can be adopted for inhomogeneous random fields. In generally, $C(\mathbf{u}_i, \mathbf{u}_j)$ is expressed by variogram $\gamma(\mathbf{u}_i, \mathbf{u}_j) = \gamma(h)$ as

$$C(\mathbf{u}_i, \mathbf{u}_j) = C(h) = \sigma^2 \exp\left(-\frac{h}{\ell}\right) = C(0) - \gamma(h) \tag{9}$$

All elements in $\mathbf{C}$ can be determined by σ^2, ℓ, and h. It should be noted that h is a known variable. The number of explanatory variables, m, in Eq. (4) is expressed as the sum of m_t, which is determined by Eq. (7), and m_c, which is the number of unknown parameters for determining $\mathbf{C}$ (i.e., $m = m_t + m_c$).

In the case of a general Kriging method, $\mathbf{z}$ is considered as a realization value in a random field. When estimating GMI from various specimens, such as boring data, non-negligible errors in estimates at the boring points must be considered. To this end, the authors proposed a modified kriging method (Sugai et al. 2015). In this method, $p(\mathbf{z}|\cdot)$ in Eq. (5) is estimated by a covariance matrix $\mathbf{C}'$, which is expressed as

$$\mathbf{C}' = \begin{bmatrix} C(\mathbf{u}_1, \mathbf{u}_1) + \sigma_1^2 & C(\mathbf{u}_1, \mathbf{u}_2) & \cdots & C(\mathbf{u}_1, \mathbf{u}_n) \\ C(\mathbf{u}_2, \mathbf{u}_1) & C(\mathbf{u}_2, \mathbf{u}_2) + \sigma_2^2 & \cdots & C(\mathbf{u}_2, \mathbf{u}_n) \\ \vdots & \vdots & \ddots & \vdots \\ C(\mathbf{u}_n, \mathbf{u}_1) & C(\mathbf{u}_n, \mathbf{u}_2) & \cdots & C(\mathbf{u}_n, \mathbf{u}_n) + \sigma_n^2 \end{bmatrix} \tag{10}$$

in which σ^2_i is the variance in the estimation error (“observation errors” (Wackernagel 2011)) of the estimates at point i, denoted $\mathbf{z}_i$. In this paper, it is assumed that $\sigma_i^2 = \sigma_c^2$ for all $i = 1, ..., n$. The number of explanatory variables in $\mathbf{C}'$, m_c, is 3, representing the explanatory variables σ^2 and ℓ of $\mathbf{C}$, and the additional explanatory variable σ_c^2.

1.3. An acceleration FS on ground surface at an arbitrary point

The acceleration FS on the surface at an arbitrary point could be estimated by the transfer function at an arbitrary point in Section 1.2 and observation records of limited number of seismometers obtained after an earthquake.

1) The acceleration FS on the engineering bedrock at seismometer points are calculated by the inverse of transfer function and the acceleration FS on the surface obtained from the observation records at the installed seismometers on the surface.
2) The coefficient vector **b** in Eq. (6) on the engineering bedrock are calculated per frequency by using the least-squares method based on the acceleration FS on the engineering bedrock at all seismometer points.
3) The acceleration FS on the surface at an arbitrary point could be estimated by the transfer function and the acceleration FS on the engineering bedrock at the same point, which is obtained from substituting the vector **b** in step 2), the latitude and longitude at the point into Eq. (6).

2. EVALUATION

2.1. Analysis of target area and data

To estimate the transfer function, the authors utilized 748 boring data in Owari-asahi City, which has an area of 21.03 km^2. Among these investigations, 676 were originally collected by Owari-asahi City Office in the 2013 fiscal year. The remainder were collected by surrounding cities. The depth of the boring data is approximately 20 m, and the depth from on the surface to the engineering bedrock in the city is assessed to be approximately 20 m based on the much longer boring data.

In the analysis, the authors utilized six earthquake scenarios from a seismic damage assessment of Owari-asahi City. The scenarios were the Sanage-Takahama fault earthquake (“Sanage-Takahama earthquake”); Tokai and Tonankai-coupled earthquake (“Coupled earthquake”); Tokai, Tonankai, and Nankai massive earthquakes (“Massive earthquakes”); and the Nankai Trough earthquakes (“Largest ever,” “Theoretical maximum-east side,” and “Theoretical maximum-land side”) (Earthquake Division of the Aichi Government's Disaster Prevention Council 2014). Seismic waveforms of the scenarios were 11 types, with one type in Sanage-Takahama earthquake and two types in others (NS and EW directions).

The seismic waveforms on the engineering bedrock were calculated for each mesh (e.g., 250 m^2) covering in the city. The seismic waves on the engineering bedrock of each boring point were estimated by the Fourier power spectra and seismic wave phases of each mesh. It was assumed that the seismic wave of each mesh was estimated at the mesh center. Then, the Fourier power spectrum at each boring point was calculated as the weighted average of the seismic waves of the four proximate meshes; the weight was given based on the square of the distance from the boring point to the center point of each mesh. The phases were assumed to be equal to those of the seismic wave of the closest mesh from the boring point.

2.2. Transfer function at boring points result

The spectral ratios of the acceleration FS on the surface to that on the engineering bedrock at each of the 748 boring points were calculated by the 11 types of seismic waves from the earthquake scenarios in Owari-asahi City in Section 2.1. Figure 2 shows each of the spectral ratios at the four boring points denoted by blue dots in Figure 1. As shown in the figures, the spectral ratios for all earthquakes excluding Sanage-Takahama earthquake were almost identical, because instrumental seismic intensity of Sanage-Takahama earthquake is larger than the others (Sanage-Takahama is 6 upper, the others is 4–6 lower). In this analysis, the transfer function at each of the boring points in the city was determined to be the logarithmic average value of the spectral ratios obtained from the 11 types of seismic waves at the same boring points.

Figure 3 shows the maximum, minimum and average of the transfer function per frequency at the 748 boring points. As shown in the figure, the values were close to one below 0.4 Hz. Although, the maximum increases and the minimum decreases as the frequency increases. It is necessary to estimate the transfer function at arbitrary points based on the spatial statistical analysis because the transfer function is different for each the boring point above 0.5 Hz.

2.3. Variogram and transfer function at arbitrary points result

Figure 4 shows the (a) AICs in Eq. (4) for the transfer functions and (b) the differences of AICs in the maximum degree zero of the trend function to the maximum degrees one and two per frequency in Owari-asahi City. As shown in the figures, the AIC was minimized when the trend function was the maximum degree zero. Therefore, the city can be represented by an optimal field model with the maximum degree zero. Figure 5 shows the range (auto-correlation distance), ℓ, and Figure 6 shows the sum of the sill, σ^2, and variance of the estimation error, σ_c^2, for each of the maximum degrees of the trend function per frequency. As shown in the figures, ℓ and $\sigma^2+\sigma_c^2$ are roughly equal to any the maximum degree, respectively.

Figure 7 shows the transfer function at arbitrary points in Owari-asahi City by using the modified Kriging method based on the variogram with the maximum degree zero of the trend function. As shown in the figures, the transfer functions are distributed between 1.0 and 1.2 for 0.6012 Hz (Figure 7(a)), 1.0 and 1.4 for 1.001 Hz (Figure 7(b)), 1.0 and 2.0 for 2.038 Hz (Figure 7(c)), and 0.6 and 2.6 for 4.065 Hz (Figure 7(d)).

2.4. An acceleration FS on ground surface at an arbitrary point using earthquake scenarios result

The acceleration FS on the surface at an arbitrary point could be estimated by using the proposed method in Section 1.3 based on the transfer function in Section 2.2 and 2.3, and observation records of limited number of seismometers. The authors assumed the installed 20 seismometers on the surface from the 748 boring points of Owari-asahi City (Figure 1, red triangles, ▲). It

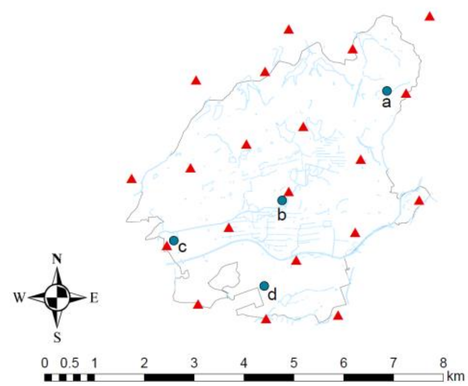

Figure 1 : Four sample boring points and assumed seismometer installation points

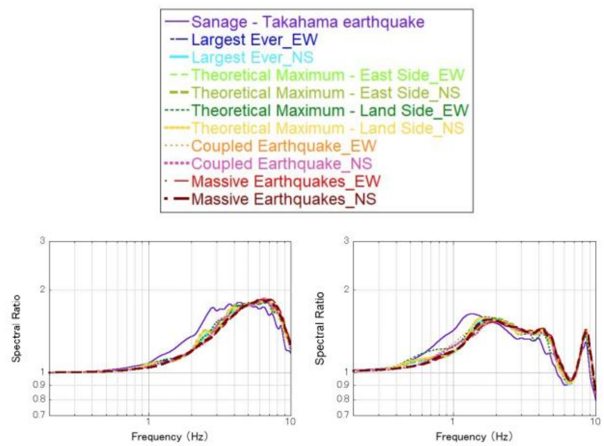

(a) Point a (b) Point b

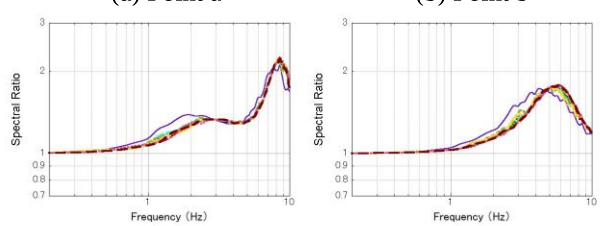

(c) Point c (d) Point d

Figure 2 : Spectral ratios at four boring points

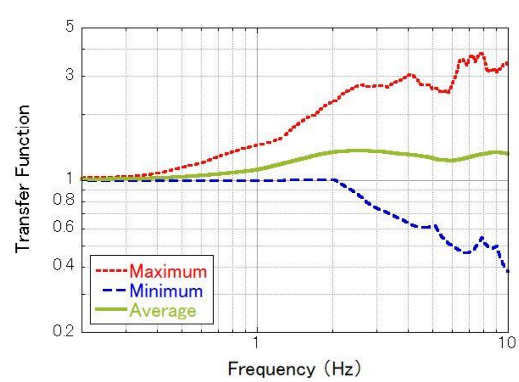

Figure 3 : Transfer functions at 748 boring points

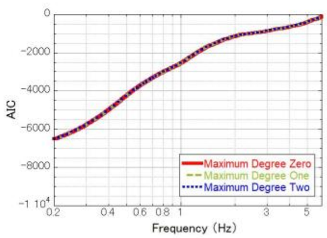

(a) AIC

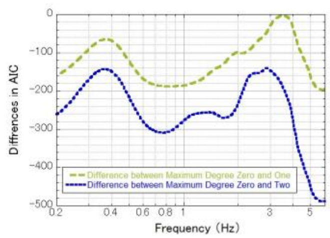

(b) Differences in AIC

Figure 4 : AIC results from modified kriging method

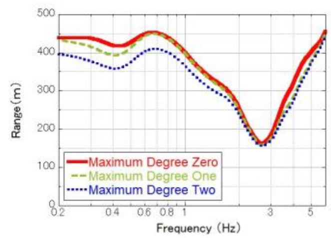

Figure 5 : Range results

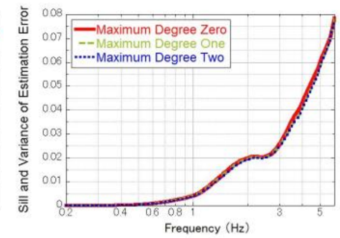

Figure 6 : Sill and variance results

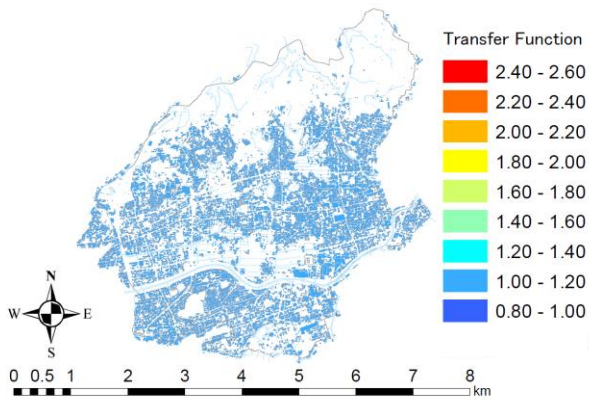

(a) 0.6012 Hz

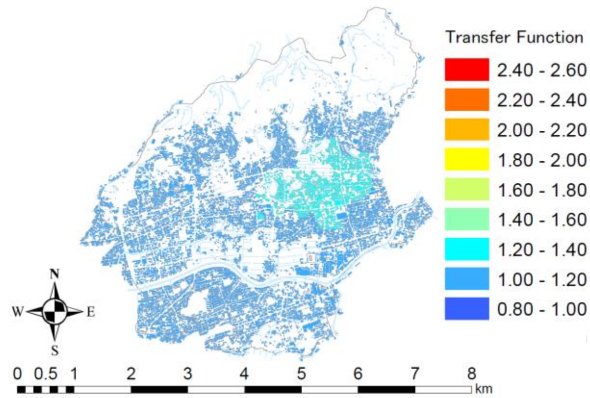

(b) 1.001 Hz

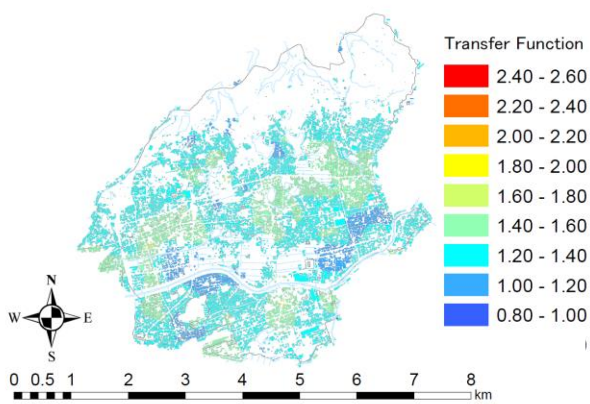

(c) 2.038 Hz

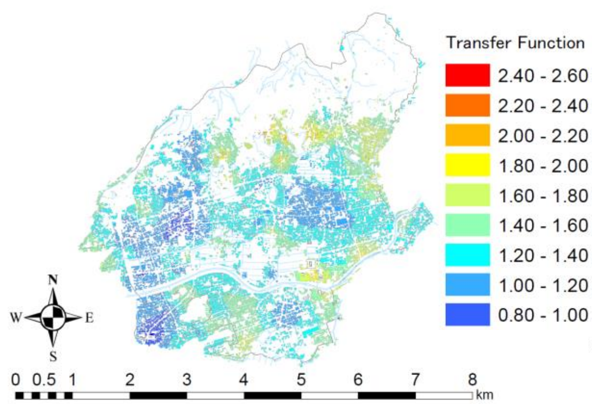

(d) 4.065 Hz

Figure 7 : Transfer function for each construction site in Owari-asahi City

was also selected 642 boring points inside the city to estimate the acceleration FS on the surface, excluding 93 points outside the city and 13 points of seismometers inside city from 748 points.

The acceleration FS on the surface at the 642 boring points were estimated by using the proposed method based on the observation records on the surface at the 20 seismometer points. Here, the observation records were assumed the value estimated by the transfer functions and seismic waves on the engineering bedrock the seismometer points from the six earthquake scenarios in Section 2.1. The **b** vector was calculated by only the maximum degree three of the trend function because the estimation of seismic damage should be performed immediately after an earthquake.

Figure 8 shows the acceleration FS on the surface estimated by using the proposed method (estimated value) and the transfer functions and the seismic waves on the engineering bedrock (tentative observed value) at four points (same points in Figure 2) for the largest ever (EW direction). As shown in the figures, the estimated and tentative observed values were almost identical.

Figure 9 shows the correlation coefficient per frequency between the estimated and tentative observed values at the 642 boring points for the six earthquake scenarios. As shown in the figures, the correlation coefficient was at least 0.5 any earthquake scenario. To improve the accuracy of the proposed method, it is necessary to perform calibration using actual observation records.

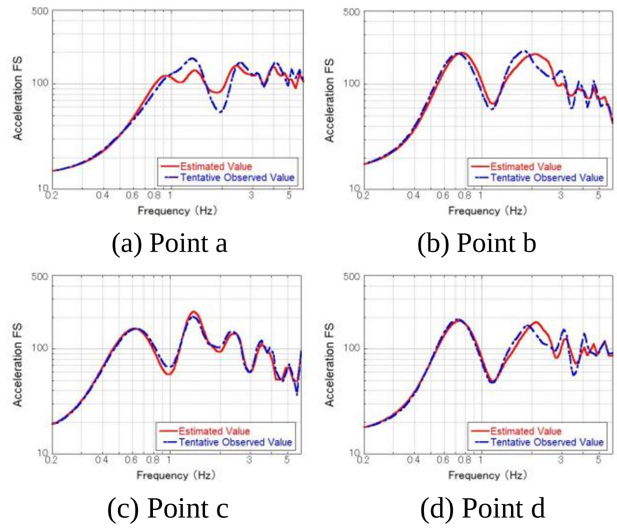

(a) Point a (b) Point b

(c) Point c (d) Point d

Figure 8 : Comparison of estimated value with tentatively observed value （largest ever, EW）

3. CONCLUSIONS

This paper reported a method for estimating an acceleration FS at an arbitrary point using transfer function which is estimated by using the modified Kriging method based on boring data and earthquake scenarios, and observation records of limited number of seismometers. The major findings of this analysis are outlined below.

1) The transfer function at an arbitrary point was estimated per frequency by using the modified Kriging method based on the transfer function at boring points, which is calculated by using the one-dimensional seismic response analysis method based on boring data and earthquake scenarios. In Owari-asahi City, it is necessary to calculate the transfer function at arbitrary points, especially high frequency ranges.

2) The acceleration FS on the surface at

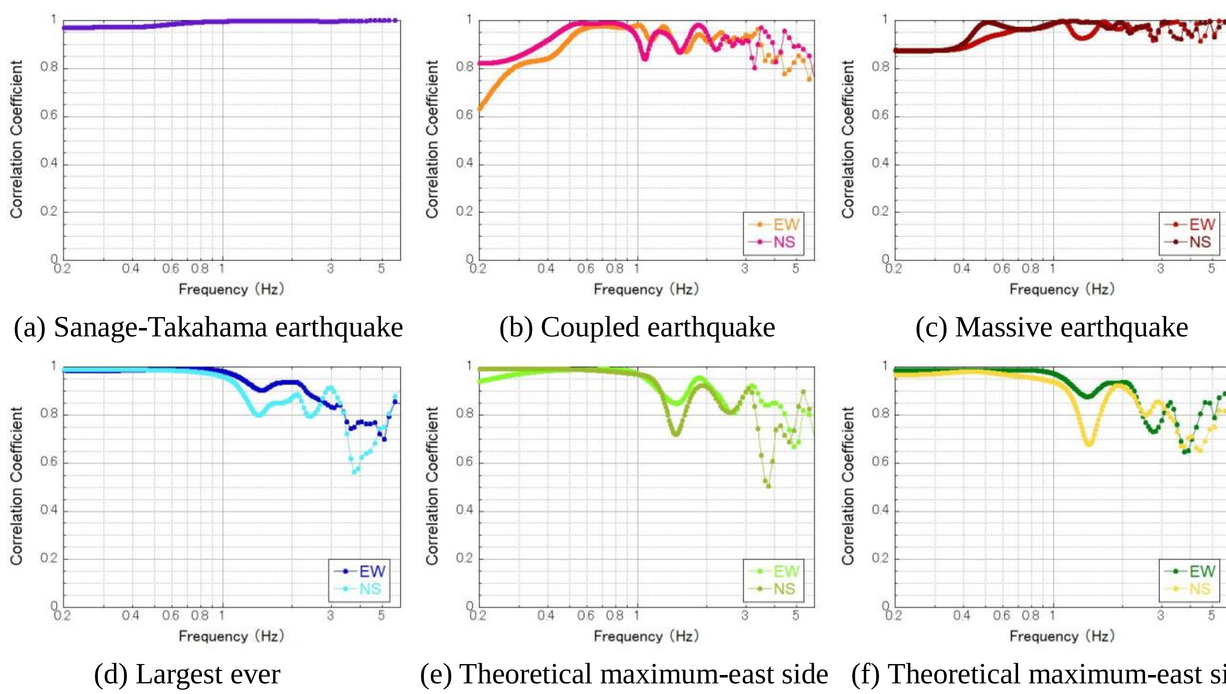

(a) Sanage-Takahama earthquake (b) Coupled earthquake (c) Massive earthquake

(d) Largest ever (e) Theoretical maximum-east side (f) Theoretical maximum-east side

Figure 9 : Correlation coefficients between estimated and tentative observed values

each of 642 boring points inside Owari-asahi City were estimated by using the proposed method based on only 20 observation records on the surface (estimated value). The results were compared to the acceleration FS estimated by transfer function and seismic wave on the engineering bedrock at the same boring points (tentative observed value). The estimated and tentative observed values were almost identical. Additionally, the correlation coefficients per frequency between the acceleration FS of the estimated and tentative observed values 642 boring points were no less than 0.5 any earthquake scenario.

If it is created a database of the transfer function per frequency at each seismometer and construction site in advance, it is possible to estimate immediately a detailed spatial distribution of the acceleration FS after an earthquake without seismic response analysis of the surface strata.

4. REFERENCES

Aichi Prefecture Disaster Council Earthquake Subcommittee. (2014). “Damage Prediction Survey Results, including Aichi Prefecture Tokai Earthquake, Tonankai Earthquake, and Nankai Earthquake in the 2011–2013 Fiscal Year.” (Japanese).

AIJ. (2015). “AIJ Recommendations for Loads on Buildings.” *AIJ*. (Japanese).

Akaike, H. (1973). “Information Theory and an Extension of the Maximum Likelihood Principle.” *2nd International Symposium on Information Theory, edited by B.N. Petrov and F. Csaki, Akad. Kiado, Budapest, Hungary*, pp. 267–281. (Japanese).

Cabinet Office, Government of Japan. (2015). “Jishinbosaimappu- sakuseigizyutusiryo (Create technical material of map of earthquake disaster).” (Japanese)

Honda, M. (2000). “Statistical Approach to Space/Time Prediction and Its Application to Geotechnical Problems.” *Doctoral thesis, Kyoto University, Japan.* (Japanese).

Imazu, M. and Fukutake, T. (1986a). “A Consideration of the Data Transactions of Dynamic Shear Moduli and Damping.” *Proceedings of the Japan National Conference on Soil Engineering*, pp. 533–536. (Japanese).

Imazu, M. and Fukutake, T. (1986b). “Dynamic Shear Modulus and Damping of Gravel Materials/” *Proceedings of the Japan National Conference on Soil Engineering*, pp. 509–512. (Japanese).

Iwata, T. and Irikura, K. (1986). “Separation of Source, Propagation, and Site Effects from Observed S-Waves.” *Earthquake 2*, vol. 39, pp. 579–593. (Japanese).

Krige, D.G. (1951). “A Statistical Approach to Some Mine Valuation and Allied Problems on the Witwatersrand” *Master’s thesis, University of Witwatersrand, South Africa.*

Matheron, G. (1963). “Principles of Geostatistics, Economic Geology.” vol. 58, pp. 1246–1266.

Mizutani, Y., Sugai, M., and Mori, Y. (2017). ”Study on the Estimation of Earthquake Ground Motion at Engineering Base Layer via Kriging Method” *Proc., Annual Meeting of Tokai Chapter*, vol. 55, pp. 189–192. (Japanese).

Sugai, M., Mizutani, Y. and Mori, Y. (2016). “Application of Kriging Method to the Estimation of Seismic Hazards for each Construction Site.” *AIJ J. Technol. Des.*, vol. 22, no. 51, pp. 447–452. (Japanese).

Sugai, M., Mori, Y., and Ogawa, K. (2015). “Application of Kriging Method to Practical Estimations of Earthquake Ground Motion Hazards.” *Journal of Structural and Construction Engineering*, AIJ, No. 707, pp. 39–46. (Japanese).

Sugito, M., Goda, H. and Masuda, T. (1994). “Frequency Dependent Equi-Linearized Technique for Seismic Response Analysis of Multi-Layered Ground.” *J.JSCE*, No.493/III-27, pp. 49-58. (Japanese).

Wackernagel, H. *Geostatistic* (2011), 3rd Edition (translated into Japanese), Morikita Shuppan.

Yoshida, N. (2010). “Earthquake Response Analysis of Ground Motion.” Kajima Institute Publishing CO., pp. 197. (Japanese).